# UAV Icing: Icing Cases for Validation of Path Planning Method

**Michael Cheung, Richard Hann, Tor Arne Johansen, Bård Nagy Stovner**
Norwegian University of Technology and Science (NTNU) Department of Engineering Cybernetics, NTNU and UBIQ Aerospace, NTNU Department of Engineering Cybernetics, UBIQ Aerospace

## Abstract

As part of the complete solution to deal with atmospheric in-flight icing on unmanned aerial vehicles (UAV), a path planner is a valuable tool for finding an optimal path for accomplishing UAV missions. When considering icing conditions, the planner manages areas with icing risk. Together with an electro-thermal ice protection system (IPS), the path planner can optimize energy consumption by comparing energy consumed flying through the cloud or around it, as the UAV can now more safely pass through the ice. The UAV's aerodynamic stability is also considered by meeting lift requirements, producing enough thrust, and having battery capacity left. These are constraints in the planner to ensure that the UAV can complete its mission. Benchmark icing cases are constructed to validate that the path planner performs as intended. A particle swarm optimization (PSO) is used as a method in the planner due to its ability to handle highly nonlinear problems and to be able to explore the solution space effectively. Weather conditions are chosen following Federal Aviation Administration 14 CFR Part 25 Appendix C icing design envelopes required for certification. A cloud with ice is designed within a defined mission area. The constructed cloud will change size between simulations, where, by a specific cloud size, the PSO predicts that less energy is consumed flying through the iced area with an IPS than flying around it. With these icing cases, a baseline is set for future validation. The work performed in this paper will be used to validate the PSO algorithm. This paper can also benefit any UAV users that require a robust path planner by using the icing cases to identify any inconsistencies in their code. The results show that one version of the PSO handles most of these icing cases well. Inconsistencies were identified when using these icing cases, but this study makes an excellent example of how they can be used.

## Introduction

In-flight atmospheric icing is a critical challenge that requires robust solutions to fully realize the potential of unmanned aerial vehicles (UAV) and urban air mobility (UAM) [1,2]. A climate report on icing risk in Norway shows 50% icing risk from October to February, meaning flight risks due to icing-related incidents is high [3,4]. Ice accretion leads to performance degradation due to changing the shape of vital aircraft surfaces, which leads to a decrease in lift, an increase in drag, and reducing the stall angle of the wings [5]. In the case of propellers, the production of thrust is reduced and can lead to instability [6]. Three main ice types can affect the wings and propeller. Glaze ice, which occurs at temperatures close to 0 °C, can have uneven surfaces and ice horns due to slow freezing. Rime ice occurs at lower temperatures, has a more streamlined shape, and has a "stickier" property. Mixed ice is a mix of these two [7].

The different types of ice also affect the wings and propeller differently. In a previous work by the authors [8], it was shown that glaze ice is the worst for aerodynamic performance degradation on the wings due to a more significant degree of distortion of the airfoil shape. Rime ice is less severe, as rime ice forms streamwise ice shapes that lead to less aerodynamic degradation. It is the opposite case for the propeller due to its rotation at high speeds, as heat builds up due to aerodynamic friction, glaze ice melts, leading to negligible performance degradation. The heat build-up due to friction is insufficient for the rime ice case as the temperatures are too low. While ice shedding is possible, rime ice is more adhesive to the propeller surface, leading to delayed shedding and larger ice shapes, which results in higher performance degradation. At the same time, rime ice has less cohesion with itself, which can lead to outer ice layers shedding first, creating uneven ice shapes that deteriorate performance further. Different propeller parts also experience different amounts of centrifugal force, with the tips experiencing the highest forces. These higher forces can first break the ice at the propeller tips, resulting in an uneven surface and worse performance. The propeller degradation is also in a different time scale than the wings. While the wings see noticeable degradation in 20 minutes, the propeller sees noticeable degradation in under a minute [6,8]. Hence, ice increases power consumption, reducing the effective operating time of UAVs, or in the worst case, can lead the aircraft to crash [9].

Unsettled icing topics were covered in the paper by Hann & Johansen [10]. Topics include developing a mature ice protection system (IPS), a better understanding of iced airfoil dynamics of wings and propellers, and path planning methods. UAVs require a path planner to manage ice-associated risks, such as performance degradation. It is possible in some cases to avoid clouds with ice conditions. However, days can occur where outright avoidance of ice is impossible. Hence, UAVs without an IPS are limited in what they can do, even with a path planner. With an IPS installed, the benefits of a path planner are twofold. The path planner can now ascertain whether flying through a cloud with ice or around it is more energy efficient. Additionally, the path planner can help optimize the use of the IPS. Since the electro-thermal IPS is an energy-intensive component of the system, knowing when to switch the IPS on or off is vital for mission success [11].

A path planner and ice detection system can help optimize IPS usage by improving efficiency and operation. As Wei et al. [12] reviewed, ice detection is possible through sensor technology or a combination of sensors and models [13–17]. The paper by Wei et al. applies to wind turbines, but the ice detection concepts can be adapted for UAVs. Research that investigates the combination of path planning, IPS, and icing effects is limited to the author's knowledge. However, one paper proposed a decision-making tool for UAVs in icing conditions that obtains environmental measurements from sensors and changes in performance due to ice to determine IPS activation

and mission success rates [18]. Although path-planning-related work explicitly aimed at icing conditions is limited, work that deals with general weather conditions does exist [19–22]. With an IPS installed, more missions are available that were previously dangerous, meaning the path planner can explore more options. To calculate the optimal path, the path planner must process weather data over its mission area. Weather datasets can be significantly large with many variables; hence a path-planning method that can deal with many variables can be more effective. One such method is particle swarm optimization (PSO) [23].

This paper proposes icing cases for validation for path planning tools. These validation cases are then used to test a pre-existing PSO path planner developed by Tiller [24], which was based on the work by Hovenburg [25] and Narum [26]. This is to showcase these icing cases and to investigate potential improvements in the PSO path planner. The paper focuses on fixed-wing UAVs; hence there will be no discussion on rotary-wing UAVs. Because of how the PSO works, it can be challenging to determine whether the planner behaves as designed. The path planning problem is also highly nonlinear due to the complex effect of terrain, clouds, icing, and IPS, which increases complexity further. A series of icing cases are developed to validate the planner's performance and consistency and to showcase its capabilities. These cases are simple enough to determine whether the best path was chosen or not quickly. These icing cases create a baseline that can be used to test new features or other algorithms. The designed icing cases will benefit UAV users that aim to optimize UAV operational uptime, minimize risk, and enable testing of their path-planning algorithms with icing conditions.

## Methods

This section presents the method for icing cases, the PSO, and the case study. The most important details of the PSO are given, and those curious about the full details are referred to the paper by Tiller [24]. The icing cases are presented in full. Lastly, the case study is presented similarly to previous work that quantified icing severity through performance degradation [8]. The wing performance curves simulated in [27], propeller performance curves calculated through simulation and experiments in [6], IPS energy consumption data in [11,28], and aircraft specifications in [29] are presented. The performance curves correspond to the airfoil, propeller, and IPS used on the Falk PX-31. Hence, the parameters used in the path planner correspond to PX-31's capabilities.

### *Icing cases*

The icing cases are designed so that it can be quickly determined whether a path planner would avoid or fly through an area with ice. The parameter of the "cloud" in the simulation is whether ice is present, a true or false value. For each case, the cloud parameters, which consist of cloud extent, air temperature, and icing condition, are artificially changed to test the PSO algorithm. These parameters are constant within the cloud. The icing conditions of the datasets are chosen per Federal Aviation Administration (FAA) icing design envelopes from CFR14, Appendix C [30]. Hence, this paper only investigates atmospheric in-cloud icing, not supercooled large droplets (SLD). The main case parameters are the different temperatures corresponding to the different ice types. −2 °C, −4 °C, and −15 °C correspond to glaze, mixed, and rime, respectively. Apart from temperature, liquid water content (LWC) is a primary factor in determining performance degradation. However, choosing an LWC must correspond with the LWC of different cloud types. The conditions adhere to the cloud extents for the continuous maximum case as specified in Appendix C [30]. For example, an increase in the horizontal area uses the LWC adjustment factor, as presented in Appendix C [30]. The lift and drag curves are also computed with Appendix C [30] in mind. The ice cases then follow the standards of the FAA design envelopes.

Two cloud types are relevant according to the FAA design envelopes, stratiform clouds and cumuliform clouds, corresponding to continuous maximum and intermittent maximum, respectively [30]. In this paper, only stratiform clouds are investigated, as stratiform clouds are the only cloud type with a possible horizontal extent relevant for the test purposes in this paper. Stratiform cloud LWC can range from 0.1–0.8 g/m$^3$. The values in the design envelopes are statistical, and with a given value, there is a chance for all values up to the given value to occur rather than being constant. For example, if a value of 0.8 g/m$^3$ is given, then all values from 0–0.8 g/m$^3$ can occur in the cloud. However, the LWC is assumed constant in the simulation to make it easier to compare. Also, as temperature decreases, the ability of air to retain moisture drops [31]. Hence, glaze ice conditions generally have higher LWC values than rime ice conditions. Larger ice shapes can occur at shorter icing durations in glaze ice conditions. The cloud's horizontal extent is also mentioned in the design envelopes. A cloud with a higher LWC generally has a lower horizontal extent, as a higher LWC can only come from its higher water concentration. Table 1 summarizes key parameters and icing cases that are explored. The designed icing cases choose only one MVD of 20 μm, as found in [8,27,28,32] to result in the highest degradation. Hence, we only simulate this MVD.

This paper ignores wind and terrain elevation as the focus is on icing effects. This means that the path planner sets wind and elevation to zero. In actual conditions, a real cloud would move from the effects of wind. This paper investigates a static cloud since it would be difficult to compare otherwise, and computational resources are currently insufficient. Currently, the weather data resolution is at 2.5 x 2.5 km. Simulating a moving cloud would require a resolution that depends on the wind speed. With a wind speed of 5 m/s, the resolution would subsequently need to upscale to capture this movement but will require an unreasonable amount of computational resources. The temperature is also constant within the cloud and does not vary with altitude. This ensures that results from different cases are comparable, and the cruising altitude is kept constant at 1800 meters. This ensures that ice is the only consideration made when comparing energy consumption. During normal runs of the algorithm, the path planner can make altitude adjustments to take advantage of air density and wind [24]. Including wind and elevation would significantly affect the outcome making it difficult to compare, and this feature is therefore disabled. The barometric formula [33] is used to estimate air density at 1800 meters.

Table 1 Icing cases and parameters for nominal continuous maximum conditions in App C [30]

| Variable | Glaze | Mixed | Rime |
|---|---|---|---|
| Temperature | −2 °C | −4 °C | −15 °C |
| Liquid Water Content | 0.60 g/m$^3$ | 0.55 g/m$^3$ | 0.33 g/m$^3$ |
| Droplet Median Volume Diameter | 20 µm | | |
| Cloud nominal horizontal extent | Stratiform: 32.2 km | | |
| Cloud maximum vertical extent | Stratiform: 2.0 km | | |

Figure 1 shows two elliptical clouds indicated by the shaded area, with the same horizontal extent at the longest dimension but with different orientations. It also shows the paths calculated by the PSO, which are discussed in the result section. The vertical extent of the cloud is assumed to extend to the ceiling of the mission space because the UAV operational limit is close to the cloud's maximum vertical extent. As the cloud's horizontal extent increases, the PSO, which tries to minimize energy consumption, will, at some point, decide it is more optimal to fly through the cloud. This is because flying around now consumes more energy than using the IPS. Clouds of different shapes and horizontal extents are also tested for a more thorough test. The profiles for the stratiform clouds include ellipses with different horizontal extents, either along the shortest path (expected to fly along the cloud) or rotated 90 degrees to block the path (expected to pass through the cloud). There are also circular clouds of different sizes. For stratiform clouds, the nominal cloud size is specified in Tab. 1. The path and energy consumption between these different clouds' shapes and ice cases are systematically compared. The different icing cases are summarized in Tab. 2. The horizontal paths of key cases are presented, while energy consumption is presented in a table for all the cases specified in Tab. 5.

Table 2 Ice case descriptions

| Case | Case description | Shape |
|---|---|---|
| Case 1 | 8.00 km radius cloud | Circular |
| Case 2 | 16.0 km radius cloud | Circular |
| Case 3 | 22.5 km radius cloud | Circular |
| Case 4 | 22.5 km radius cloud | Elliptical, 90-deg to the path |
| Case 5 | 22.5 km radius | Elliptical, along the path |
| Case 6 | 16.0 km radius | Elliptical, 90-deg to path |

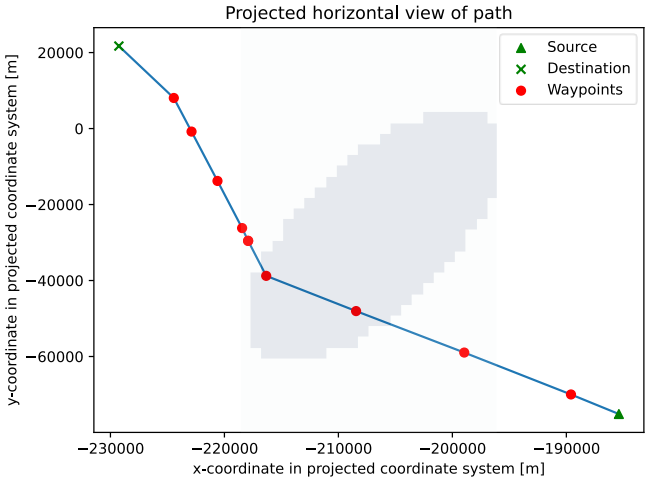


Figure 1.a. Case 4, 90 degree to the path, −2°C

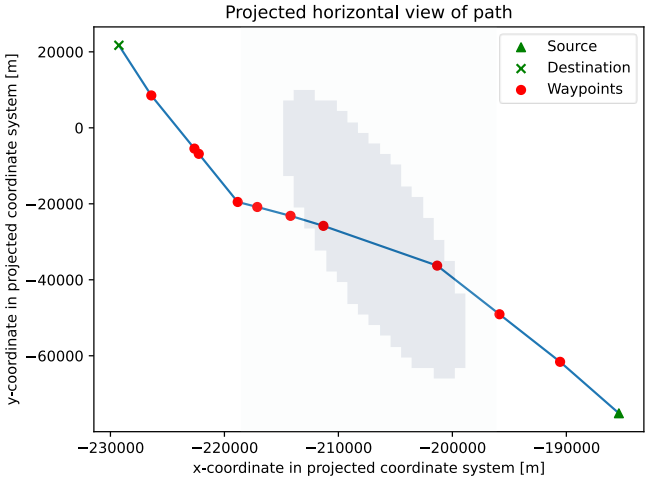


Figure 1.b. Case 5, Along the path, −4°C

Figure 1 An example of a cloud from the icing cases and resulting path.

## *Particle Swarm Optimization*

The path planner simulates realistic conditions to calculate the best path using PSO [24]. As the name suggests, the PSO method initializes a swarm of particles to explore the mission area. In the path planner, the start and end destination are user specified. Each particle contains weather data of the point in space it occupies, and UAV states such as position, velocity, acceleration, and orientation, which are updated from the previous UAV state. Weather data can be pulled from the Norwegian meteorological institute (MET). This paper replaces the MET data with the icing case data. During normal operation of the planner, ice condition is classified using relative humidity (larger than 0.99), air temperature (negative temperature), and LWC (larger than 0.01 g/m$^3$). The icing cases use the data format from MET as a template. The dataset has limited resolution, and data between grid nodes must be interpolated, which can be inaccurate as weather conditions can be complex [31]. A higher resolution is available but will increase the runtime of the PSO. Variables such as

temperature and liquid water content (LWC) are vital in determining icing severity [34]. Generally, the higher the LWC, the more severe icing becomes. Figure 2 shows the general setup of the PSO algorithm.

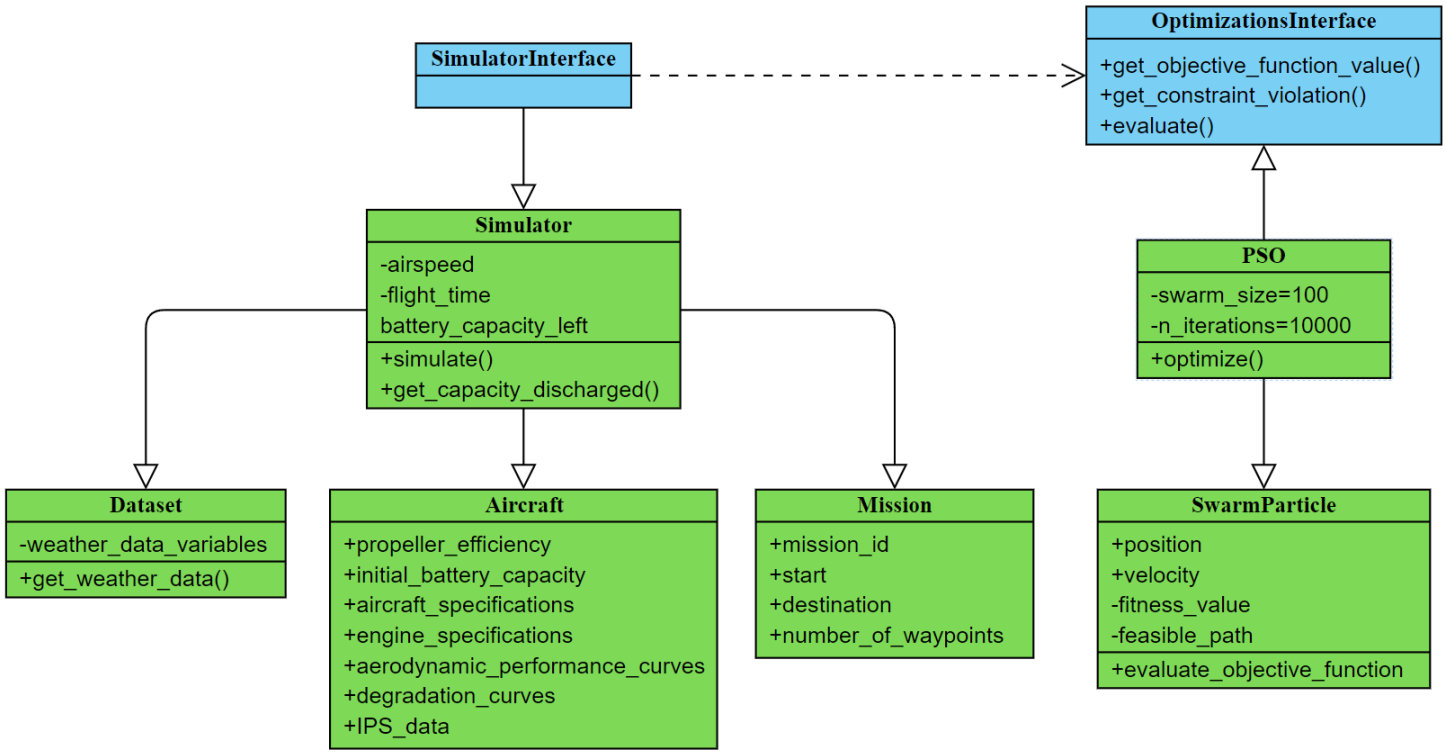


Figure 2 Unified modelling language (UML) diagram of the PSO algorithm, a common way to show relations between classes in an algorithm. The solid arrows represent association. For example, the simulator box contains references to each of the bottom three green classes. The striped arrow is an implementation. The arrows can be flipped to represent input/output. The bottom three green boxes can be seen as inputs to the simulator, with attributes sent as input into the simulator described in the boxes. The particle box can be seen as an input to the optimizer. The PSO box sends an optimization call with specified swarm size and iterations such that the particle box starts searching the space. Adapted from [24].

The objective can be user-specified to minimize energy consumption or time taken. The general constrained optimization formulations, as given in Tiller [24], are as follows:

$$\min_{p} f(p)$$

$$subject\ to\ p_{1,i} \le p_i \le p_{u,i}, \qquad i = 1, \dots, n_p$$

$$c_i(p) \le 0, \qquad i = 1, \dots, n_c$$

where the function f is the objective function to be minimized (energy or time). Input $p$ to the function are decision variables that change depending on what is being minimized. $p_{1,i}$ and $p_{u,i}$ are the decision variables' lower and upper bounds, respectively. $n_p$ and $n_c$ are number of decision variables and constraints, respectively. Lastly, $c_i$ are functions defining inequality constraints given the decision variable $p$ as an input. The PSO tries to minimize the objective function given these constraints. The constraints include battery capacity considerations; for example, the battery should not be empty before reaching the destination. Additionally, the UAV should never hit terrain; hence UAV altitude must be higher than the terrain elevation. Also, the flight path angle must not exceed some value between waypoints to ensure a flyable path, and ground speed must be positive to ensure progress. Lastly, the horizontal waypoint distance must be constrained so the path is realistic. These are the functions that the PSO tries to solve. For a more detailed problem description, consult Tiller's paper [24].

Tuning parameters include the number of particles, number of iterations, and number of waypoints. The more particles, the more the mission space can be explored, but with a penalty on computational resources. A waypoint is a series of points a vehicle must pass through toward its destination. The number of waypoints determines the resolution of the path. The more waypoints were chosen, the smoother the path becomes, at the expense of computational time. In this paper, the number of waypoints is set to ten. The particles explore sequentially from waypoint to waypoint. The particle swarm finds the optimal route by calculating the power at a point in space from the previous waypoint and then places a new waypoint where this is the lowest. The planner tracks the individual and local best particles regarding energy consumption. The local particle then functions as an attractor for every other particle. This is repeated between iterations. This attraction principle is used because UAV maneuvering capabilities need to be satisfied. The individual best is tracked to maintain the velocity direction within an acceptable range [35].

One problem with the PSO is that the particles used to explore the space require a seed for consistent comparison. Hence, the PSO must be more exhaustive in its search for an optimal global route. It can be exhaustive, but this incurs a heavy cost in computational power as more particles must be included. In most cases, the calculated route might only be a local optimum. However, the global best route is not always needed if the priority is mission completion. The PSO can optimize in terms of energy or time. However, for this paper, optimizing for time would not make sense if ice were the only consideration, as it would always take the fastest route without regard

to energy consumption. The PSO does not yet consider the flyability of the path, i.e., it does not consider the dynamics of the UAV. This is because of the resolution of the weather data. The spatial resolution is 2.5 km x 2.5 km. The UAV can follow any number of paths between waypoints that can satisfy its dynamics. After a path has been calculated, post-processing is possible to ensure a flyable path.

For each particle's candidate solution path, the power consumption to reach the next waypoint is calculated by calculating the required thrust to overcome the drag and IPS power if an icing condition is present. It is assumed that the required power depends on how much thrust the propeller needs to generate to maintain constant velocity and altitude. The lift, drag, and propeller efficiency determines the power requirement. As ice becomes more severe, the lift generation and propeller efficiency decrease and drag increases, making it more difficult to maintain steady flight. Propeller efficiency is complex as it can fluctuate due to the continuous accretion and shedding events, as the centrifugal forces can lead to ice shedding. A more detailed discussion can be found in [8]. However, since the desired outcome is determining if the PSO algorithm is making the right decisions, an IPS is used to prevent severe icing impact. Comparing the ice-free flight around an area with ice and flying straight through with an IPS can determine which is more energy efficient. The iced wing and IPS energy consumption data come from numerical modelling and icing wind tunnel tests (IWT) as described in various papers [9,11,36].

An IPS can be operated in two modes, anti-icing and de-icing. Anti-icing aims to prevent ice from forming, hence requiring higher energy consumption. De-icing allows some ice to form on the surface before it is periodically removed, leading to performance degradation. However, it needs to compensate with an increased heat flux delivered to the heating elements the longer this cycle becomes. In this paper, this de-icing cycle is set to 4 minutes, as it is concluded in [11] that 4 minutes is optimal.

This paper assumes that the propeller always uses anti-icing mode during icing conditions. This is because of how fast propeller performance degrades and how detrimental the degradation is when it happens. In one minute, it is possible to lose up to 80% efficiency [6]. However, it is not easy to say whether this is enough for the UAV to become inoperable and crash since the high rotational rate of the propeller can lead to ice shedding [36]. For the wings, the degradation is less severe timewise. Hence, the de-icing mode is used for the wings. One important thing to note is that the PSO has quite a few simplifications to make it calculate a path fast enough, such as using a simple lift/drag model for the UAV. These simple models are lift and drag curves for a specific airfoil at different icing conditions. Ice accumulation is assumed to be linear with time. Lift and drag curves for unsimulated ice conditions are linearly interpolated from existing curves. For example, we interpolate using −4 °C and −10 °C curves if the temperature is −6 °C. LWC and MVD are also a factor. Hence, trilinear interpolation must be used.

To specifically highlight the IPS model in the PSO, it is assumed that the IPS manages to shed ice perfectly, meaning that all ice gets cleared per cycle. This is not the case in real life due to run-back icing, as only part of the wing has heating elements. Heating loads are directly proportional to the area of the heated wing. One way to make IPS operations more efficient is to leverage aerodynamic forces by heating the leading edge with a parting strip IPS. This creates a gap that allows airflow access and hence apply aerodynamic forces to shed the ice. Full detail on this design is available in [32]. Run-back icing is the refreezing of droplets towards the wing's trailing edge. Intercycle effects happen between turning the IPS on and off during de-icing mode covered in [32]. The important main effect in this paper is the performance degradation due to ice build-up on the wing for 4 minutes. The data relating to performance degradation, IPS, and general characteristics are now presented as a case study of the PX-31 Falk in the next section.

## *Case study: PX-31 Falk*

Maritime Robotics developed the PX-31 Falk and is a fixed-wing UAV with a propeller propulsion system. The airfoil is RG-15. Table 3 summarizes key specifications. The iced wing and propeller curves are simulated through ANSYS FENSAP-ICE [6,27]. As a side note, the airspeed of the UAV affects water catch rates and needs to be specified. The performance curves are generated considering constant airspeed of 25 m/s, the same as the cruise speed of the Falk. The performance degradation is assumed to degrade linearly between the clean case and the degradation curve for a given meteorological condition. The propeller and wing profile used in the numerical simulation is the same as the Falks. Hence, the lift and drag curves for the RG-15 and propeller efficiency are mainly the data included in the PSO. The wing is simulated under Appendix C conditions, from −2 to −40 °C, for 15-50 μm MVD. This paper performs the simulations in ice conditions as presented in the icing case section. The propeller is simulated from −2 to −15 °C.

Experiments show that IPS power consumption for rime ice is eight times higher than glaze ice, as shown in Tab 4. Table 4 shows the IPS power requirements for the propeller and wings. The difference between the power requirements between anti-icing and de-icing can be observed. Although it has been mentioned earlier that icing rates depend on LWC, the IPS power requirements depend only on temperature. This is because an electro-thermal IPS functions by melting the interface between the ice and the aircraft surface. Once the interface has melted and a liquid film is created, the ice can then slide off and shed due to aerodynamic forces, irrespective of the amount of ice accreted. In theory, a thicker ice layer would result in a higher applied aerodynamic force on the ice, leading to quicker shedding but is not considered in the study [9]. Hence, IPS power requirements only depend on the power needed to heat the aircraft surface to a temperature above zero, which only depends on the ambient temperature [11].

For the propeller IPS, the power requirement is calculated typically on a per-second basis. The power requirement for the wing IPS de-icing mode is averaged based on the 4-minute de-icing cycle. The IPS is usually only on for a short period. Meaning in those 4 minutes, the IPS consumes some energy. The power is then calculated by dividing the energy consumed by 4 minutes to get an average power consumption. The data presented here are used in the PSO for path optimization and to validate its behavior.

Table 3 PX-31 Falk Specifications [29]

| | |
|---|---|
| Aircraft mass (max take-off weight) | 25 kg |
| Standard operating weight | 18 kg |
| Cruise speed | 25 m/s |
| Max speed | 40 m/s |
| Wing surface area | 0.6 $m^2$ |
| Wingspan | 3.2 m |
| Engine efficiency | 0.8 |
| Clean propeller efficiency | 0.68 |
| Operational ceiling | 2300 m |

Table 4 IPS power requirements at different temperatures for propellers and wings

| Variable | Glaze | Mixed | Rime |
|---|---|---|---|
| Temperature | −2 °C | −4 °C | −15 °C |
| Propeller anti-icing IPS power [6] | 50 W | 83 W | 400 W |
| Wing de-icing IPS power [11] | 12 W | 29 W | 69 W |

In the next section, the results are presented and discussed. The main results with circular-shaped clouds are presented in their entirety. The elliptically shaped cloud cases are available to the interested reader in the appendix.

## Results and Discussion

This section presents the calculated horizontal profile for cases 1–3, for −2 °C, −4 °C, and −15 °C in that order. The energy consumed for cases 1–6 is shown in Tab. 5 for comparison purposes. The interested reader can find the horizontal profile for cases 4–6 in the appendix.

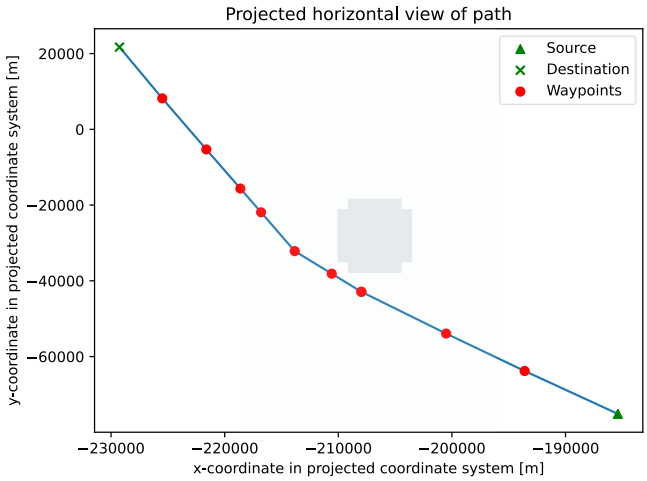


Figure 3 Case 1 for −2 °C

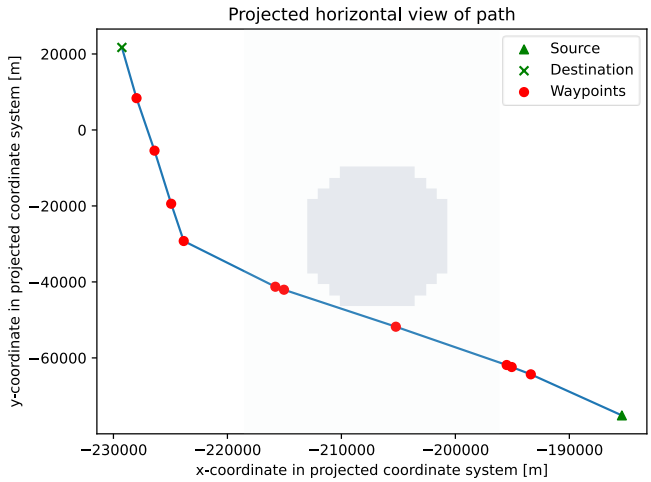


Figure 4 Case 2 for −2 °C

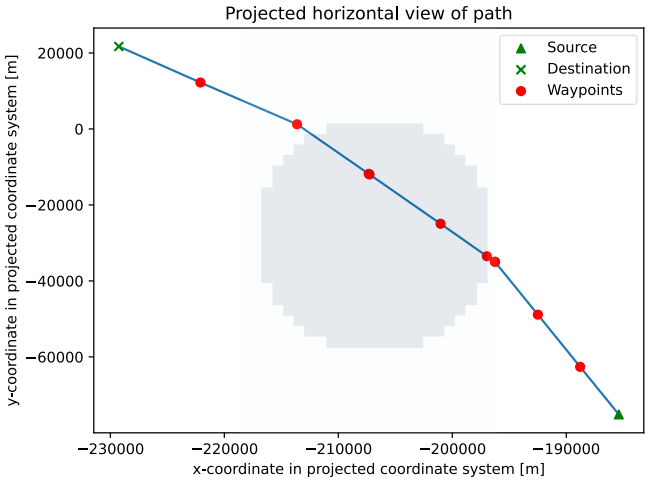


Figure 5 Case 3 for −2 °C

Figure 3–5 shows the paths for −2 °C. For cases 1–2, the computed paths are as expected, flying around the cloud. This is due to the small cloud extent. For case 3, the computed path passes through the cloud, as flying around the cloud would cost more energy. Why the horizontal paths are not entirely the same, although the cloud size is the same for the same cases, but with different parameters, is due to how the particles search the space stochastically. It leads to similar, but not identical, paths. The Figs. 6–11 showing cases 1–2 for the other temperatures give similar results of flying around. However, for case 3, the calculated path shows that the best path is flying around the cloud. This might be because the IPS power requirements are significantly higher for the −15 °C case, as the propeller IPS power quadruples and more than doubles for the wing IPS compared to the −4 °C case. This makes the path planner consider the way around the optimal route in terms of energy optimization.

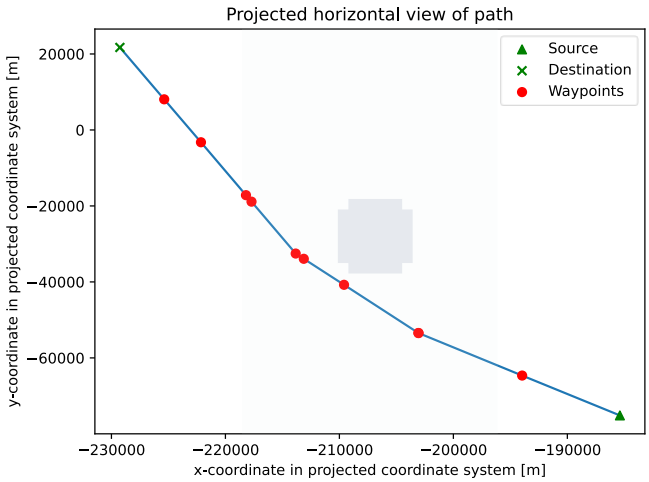


Figure 6 Case 1 for −4 °C

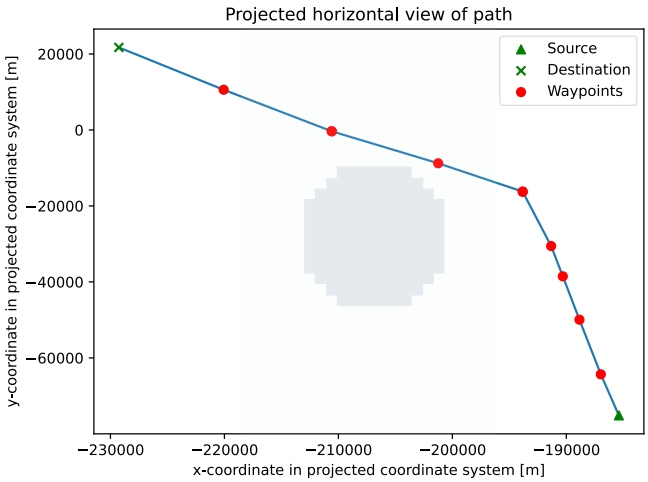


Figure 7 Case 2 for −4 °C

There are still some issues when looking at Figures 8 and 11, as the path sometimes intersects the cloud. This is a known problem that is discussed in [24]. The path between waypoints has constant conditions. For example, when considering one waypoint, the conditions at that waypoint and path are fixed until the next waypoint. However, when comparing Figures 8 and 11, it is possible to observe that the path planner could be better and has limits to its search capabilities given the PSO parameters specified in the methods section. In Fig. 11, one waypoint is set within the cloud, which is not consistent when compared with Fig. 8. The condition in Fig. 8 has a lower IPS power requirement than the conditions in Fig. 11, which should indicate that the path planner would make sure to avoid the cloud even more. However, the opposite happens, which might indicate that the stochastic nature of the planner can give sub-optimal paths, even when a better path exists in proximity when comparing these two figures. However, it is not confirmed that the algorithm's stochastic nature leads to this issue; it is only a hypothesis.

In contrast to what is stated in the PSO section on constraints, it is possible to observe waypoints that are close to each other in many figures. Given that the constraints are defined trying to make the waypoints' horizontal distance as evenly distributed as possible, this closeness between waypoints is inconsistent and should be investigated further. Another area for improvement can be observed in several figures, such as Figs. 8, 11, and 12, where detours are taken once the cloud is circumvented, rather than taking the shortest path towards the destination. It may be the stochastic nature of the PSO, or some heuristics are required, such as the shortest path being taken. In any case, it is something that should be investigated.

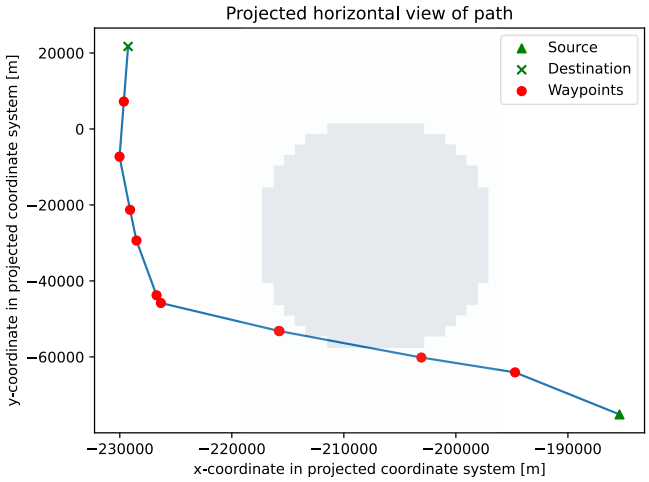


Figure 8 Case 3 for −4 °C

Although the calculated paths from the PSO are not entirely as expected, it highlights that the design cases are working as intended. The icing cases are simple enough to spot inconsistencies. When making these icing cases, there were a few inconsistencies in the results, which led to identifying some underlying issues in the PSO path planner code. This resulted in discovering some problems that needs to be handled and that would otherwise not have been detected. The statement that these problems would not have been detected is because of the magnitude of weather data. The weather dataset must be painstakingly searched and compared to the path to find inconsistencies. This would have been time-consuming and not the most effective way to identify problems. With the icing cases, identifying potential issues is now easier.

The elliptical paths in Fig. 1 and all the along-path elliptical clouds in the appendix do not choose to fly along the cloud, but at some point, they even fly through it, with waypoints set in the cloud. This requires further investigation. One major issue is that in some cases, even when the PSO has a waypoint in the middle of the cloud, the icing condition is not registered. Since this is critical in determining

the path, it is crucial to solve this issue. It is, at this moment, unknown why this occurs, but it is hypothesized to be a discretization issue. The way the cloud is coded in the PSO is a Boolean value, true or false. The PSO interpolates values between the nodes, which can mean that when interpolating Boolean values might result in wrong cloud values. However, this problem occurs sporadically and is not uniform across different conditions, as shown in figures in the appendix, such as Figs. 16 and 18. In these two figures, ice condition is only registered once or twice, which leads to a path that unnecessarily prolongs ice exposure. It is possible to observe that it depends on the cloud's shape and size. The computed paths where the cloud is avoided do not have this issue. There may be an issue with how waypoints are set and how icing condition is registered. Icing conditions are registered in an array the same size as the number of waypoints. The waypoints and array then correspond to each other. However, there might be some issues with how this is handled in the algorithm. Hence, further investigation is required.

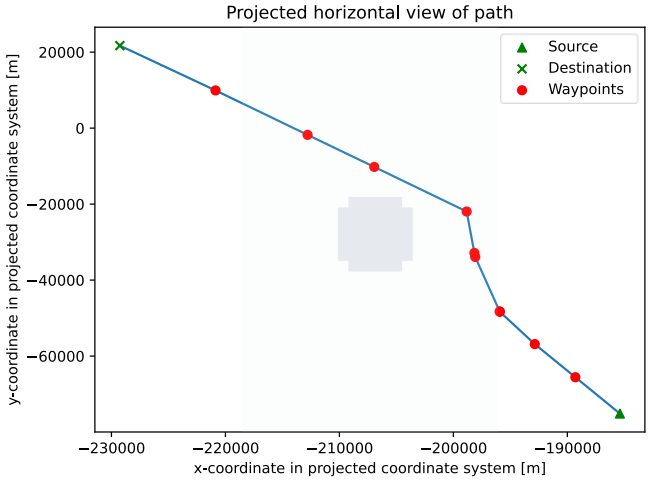


Figure 9 Case 1 for −15 °C

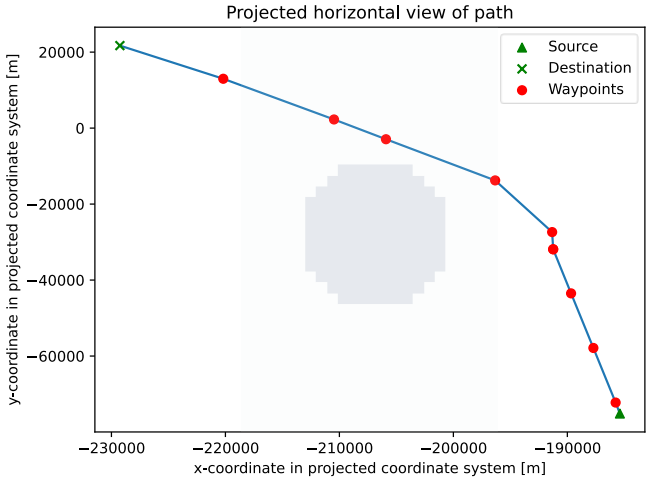


Figure 10 Case 2 for −15 °C

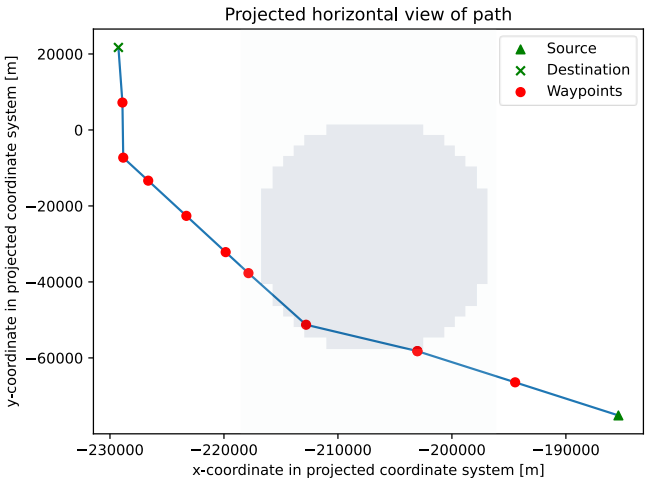


Figure 11 Case 3 for −15 °C

Table 5 compares the energy consumption for the different cases. For cases 1 and 2, the energy consumed is mostly the same for all temperatures, which is a good indication that the planner is working as intended for these cases. The −15 °C cases consume more energy when flying through a cloud due to its much higher IPS power requirements. The −4 °C cases also consume more energy than the −2 °C cases. Otherwise, the minor differences are due to PSO variations in cases where the PSO calculates paths that avoid ice altogether.

Table 6 compares the energy consumed when flying through and around the cloud for the −4 °C and −15 °C, and Figs. 12 and 13 show the paths. The table shows for these cases that flying around is optimal for minimizing energy consumption. This shows the importance of optimizing the IPS power consumption, as it is an energy-intensive part of the system. If a mission is time-sensitive, flying through a cloud might be the fastest route. If the IPS consumes as much power as indicated in Tab. 3, mission success rates would inevitably drop due to insufficient battery capacity. Lastly, the placement of waypoints is irregular, and one would expect them to be more evenly spaced. However, this might be because the PSO calculates a path requiring a smoother path at some points, and two waypoints are put close together. To include more waypoints in the simulation and get a more accurate path is planned for future work. The icing cases have then been shown to help identify issues in the underlying PSO code and has helped in improving the algorithm. These cases can be used in the future when expanding the code.

Table 5 Summary of energy consumption for the different cases and temperatures

| | **Case 1** | **Case 2** | **Case 3** | **Case 4** | **Case 5** | **Case 6** |
|---|---|---|---|---|---|---|
| **−2 °C** | 2.31Ah | 2.42Ah | 3.01Ah | 3.03Ah | 2.57Ah | 2.61Ah |
| **−4 °C** | 2.31Ah | 2.42Ah | 3.45Ah | 3.43Ah | 2.73Ah | 2.65Ah |
| **−15 °C** | 2.33Ah | 2.42Ah | 6.48Ah | 4.38Ah | 3.80Ah | 3.63Ah |

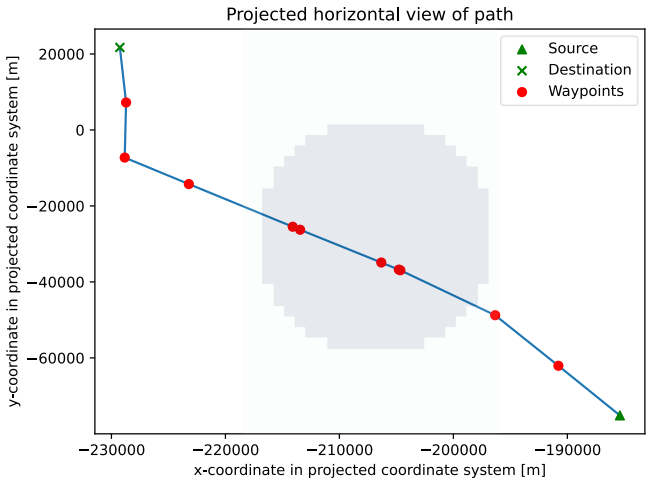


Figure 12 Horizontal path through the cloud for case 3 for −4 °C

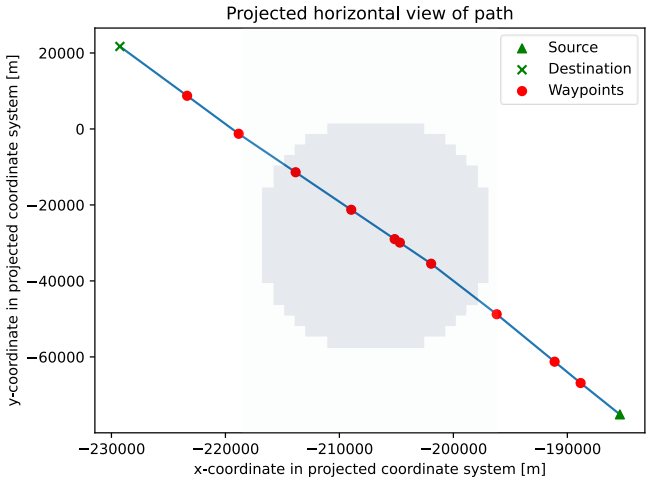


Figure 13 Horizontal path through the cloud for case 3 for −15 °C

Table 6 Comparison between flying around and through the cloud for case 3 for meteorological conditions specified in the table below.

| | **Flying through cloud** | **Flying around cloud** |
|---|---|---|
| **-4 °C** | 3.75 Ah | 3.45 Ah |
| **-15 °C** | 7.01 Ah | 6.48 Ah |

## Conclusions

In this paper, we presented icing cases, and a PSO path planner and used model data from the PX-31 Falk UAV as a case study for path planning validation. The developed icing cases aim to be as simple as possible to be able to quickly identify if the path calculated is what is reasonably expected. Clouds of different sizes and shapes were constructed to achieve this. One would expect the path planner to calculate a path around the smaller clouds while flying through the cloud when it gets big enough. The threshold of flying through vs. flying around is when the energy consumption of flying around the cloud exceeds flying through the cloud. Three ambient temperatures representing the three ice types of glaze, mixed and rime ice, were tested for six cases. Each case represents a cloud of different sizes, shapes, and orientations. These icing cases and the PX-31 Falk data were input to the PSO to generate paths. It was shown that flying around the cloud would be more energy efficient for the two lower temperatures when the cloud is at its longest extent because of how high the IPS power consumption becomes at lower temperatures. This shows the need to make electro-thermal IPS more efficient. That flying around is correct is also validated by comparing the energy consumed. By using these icing cases, some inconsistencies in the code were identified and further investigated. This shows that the icing cases are fulfilling their purpose. This can benefit UAV users that require robust path planners and can be used as a tool to validate their algorithms.

## Future Work

For future work, the identified issues will be dealt with, as presented in the results when using icing cases. The icing cases must also be tested with wind and altitude changes to gain more insight into how the PSO path planner behaves. The PSO also needs to be modified to account for altitude change better, as energy considerations due to altitude are currently not accurate enough. Additionally, some heuristics should be introduced to deal with some detours the PSO simulates. The straight path is optimal if there are no obstacles to the destination. Lastly, modifications dealing with the correct registration of icing conditions and the number of waypoints and particles must be investigated. Up-to-date propeller data will also be implemented.

For new implementations, as the UAV periodically flies through icing conditions, it becomes increasingly uncertain how much ice the IPS removes since the IPS does not manage to remove all ice perfectly. An accumulative penalty should be applied for each encounter with ice to account for this imperfect ice shedding. Additionally, aircraft elevator data will be implemented to implement a stability criterion in the path planner. The implementation of dynamics in the planner is planned, as static and dynamic stability as a constraint is of interest. The usage of higher-resolution data is planned to compare computational performance. Lastly, decision-making theory will be implemented in the path planner to allow the UAV to decide the course of action when the uncertainty of icing conditions becomes too high during flight.

## Acknowledgments

The Research Council of Norway partly sponsors the work through the Centre of Excellence funding scheme, project number 223254, AMOS, IPN project number 296228, and ITKPLUSS. Thanks to Maritime Robotics for the Falk data.

## References

[1] Cohen, A. P., Shaheen, S. A., and Farrar, E. M. “Urban Air Mobility: History, Ecosystem, Market Potential, and Challenges.” *IEEE Transactions on Intelligent Transportation Systems*, Vol. 22, No. 9, 2021, pp. 6074–6087. https://doi.org/10.1109/TITS.2021.3082767.

[2] Gao, M., Hugenholtz, C. H., Fox, T. A., Kucharczyk, M., Barchyn, T. E., and Nesbit, P. R. “Weather Constraints on Global Drone Flyability.” *Scientific Reports*, Vol. 11, No. 1, 2021. https://doi.org/10.1038/s41598-021-91325-w.

[3] Sørensen, K. L., Borup, K. T., Hann, R., Bernstein, B. C., and Hansbø, M. “UAV Atmospheric Icing Limitations: Climate Report for Norway and Surrounding Regions.” 2021.

[4] Bernstein, B. C., and Le Bot, C. “An Inferred Climatology of Icing Conditions Aloft, Including Supercooled Large Drops. Part II: Europe, Asia, and the Globe.” *Journal of Applied Meteorology and Climatology*, Vol. 48, No. 8, 2009. https://doi.org/10.1175/2009JAMC2073.1.

[5] Bragg, M. B., Broeren, A. P., and Blumenthal, L. A. “Iced-Airfoil Aerodynamics.” *Progress in Aerospace Sciences*, Vol. 41, No. 5, 2005, pp. 323–362. https://doi.org/10.1016/j.paerosci.2005.07.001.

[6] Müller, N. C., and Hann, R. “UAV Icing: A Performance Model for a UAV Propeller in Icing Conditions.” *AIAA AVIATION 2022 Forum*, American Institute of Aeronautics and Astronautics, 2022.

[7] Hann, R., and Johansen, T. A. “UAV Icing: The Influence of Airspeed and Chord Length on Performance Degradation.” *Aircraft Engineering and Aerospace Technology*, Vol. 93, No. 5, 2021, pp. 832–841. https://doi.org/10.1108/AEAT-06-2020-0127.

[8] Cheung, M., Hann, R., and Johansen, T. A. “UAV Icing: A Unified Icing Severity Index Derived from Performance Degradation.” *AIAA AVIATION 2022 Forum*, American Institute of Aeronautics and Astronautics, 2022.

[9] Hann, R. *Atmospheric Ice Accretions, Aerodynamic Icing Penalties, and Ice Protection Systems on Unmanned Aerial Vehicles. PhD Thesis*. Norwegian University of Science and Technology, 2020.

[10] Hann, R., and Johansen, T. A. “Unsettled Topics in Unmanned Aerial Vehicle Icing.” *SAE EDGE*, 2020. https://doi.org/10.4271/EPR2020008.

[11] Wallisch, J., and Hann, R. “UAV Icing: Experimental Investigation of Ice Shedding Times with an Electrothermal De-Icing System.” *AIAA AVIATION 2022 Forum*, American Institute of Aeronautics and Astronautics, 2022.

[12] Wei, K., Yang, Y., Zuo, H., and Zhong, D. “A Review on Ice Detection Technology and Ice Elimination Technology for Wind Turbine.” *Wiley Wind Energy*, Vol. 23, No. 3, 2019, pp. 433–457. https://doi.org/10.1002/we.2427.

[13] Cristofaro, A., Johansen, T. A., and Aguiar, A. P. “Icing Detection and Identification for Unmanned Aerial Vehicles Using Adaptive Nested Multiple Models.” *International Journal of Adaptive Control and Signal Processing*, Vol. 31, No. 11, 2017, pp. 1584–1607. https://doi.org/10.1002/acs.2787.

[14] Løw-Hansen, B., Hann, R., and Johansen, T. A. “UAV Icing: Ice Shedding Detection Method for an Electrothermal De-Icing System.” *AIAA AVIATION 2022 Forum*, 2022.

[15] Hansen, S., and Blanke, M. “Diagnosis of Airspeed Measurement Faults for Unmanned Aerial Vehicles.” *IEEE Transactions on Aerospace and Electronic Systems*, Vol. 50, No. 1, 2014. https://doi.org/10.1109/TAES.2013.120420.

[16] Ducard, G., Rudin, K., Omari, S., and Siegwart, R. “Strategies for Sensor-Fault Compensation on UAVs: Review, Discussions & Additions.” *2014 European Control Conference, ECC 2014*, 2014.

[17] Ying, S. Bin, Ge, T., and Ai, J. L. “H ∞ Parameter Identification and H 2 Feedback Control Synthesizing for Inflight Aircraft Icing.” *Journal of Shanghai Jiaotong University (Science)*, Vol. 18, No. 3, 2013. https://doi.org/10.1007/s12204-013-1401-6.

[18] Armanini, S. F., Polak, M., Gautrey, J. E., Lucas, A., and Whidborne, J. F. “Decision-Making for Unmanned Aerial Vehicle Operation in Icing Conditions.” *CEAS Aeronautical Journal*, Vol. 7, No. 4, 2016, pp. 663–675. https://doi.org/10.1007/s13272-016-0215-2.

[19] Thibbotuwawa, A., Bocewicz, G., Radzki, G., Nielsen, P., and Banaszak, Z. “UAV Mission Planning Resistant to Weather Uncertainty.” *Sensors (Switzerland)*, Vol. 20, No. 2, 2020. https://doi.org/10.3390/s20020515.

[20] Kamgarpour, M., Dadok, V., and Tomlin, C. “Trajectory Generation for Aircraft Subject to Dynamic Weather Uncertainty.” *Proceedings of the IEEE Conference on Decision and Control*, 2010, pp. 2063–2068. https://doi.org/10.1109/CDC.2010.5717889.

[21] Rubio, J. C., Vagners, J., and Rysdyk, R. “Adaptive Path Planning for Autonomous UAV Oceanic Search Missions.” *Collection of Technical Papers - AIAA 1st Intelligent Systems Technical Conference*, Vol. 1, No. September, 2004, pp. 131–140. https://doi.org/10.2514/6.2004-6228.

[22] Rubio, J. C. *Long Range Evolution-Based Path Planning for UAVs through Realistic Weather Environments*. University of Washington, 2004.

[23] Eberhart, R., and Kennedy, J. “New Optimizer Using Particle Swarm Theory.” *Proceedings of the Sixth International Symposium on Micro Machine and Human Science*, 1995, pp. 39–43. https://doi.org/10.1109/MHS.1995.494215.

[24] Tiller, M. *Path Planning for Fixed-Wing UAVs in Wind and Icing Conditions. Master Thesis*. Norwegian University of Science and Technology, 2021.

[25] Hovenburg, A. R., de Alcantara Andrade, F. A., Hann, R., Rodin, C. D., Johansen, T. A., and Storvold, R. “Long-Range Path Planning Using an Aircraft Performance Model for Battery-Powered SUAS Equipped With Icing Protection System.” *IEEE Journal on Miniaturization for Air and Space Systems*, Vol. 1, No. 2, 2020, pp. 76–89. https://doi.org/10.1109/jmass.2020.3003833.

[26] Narum, E., Hann, R., and Johansen, T. A. “Optimal Mission Planning for Fixed-Wing UAVs with Electro-Thermal Icing Protection and Hybrid-Electric Power Systems.” *2020 International Conference on Unmanned Aircraft Systems, ICUAS 2020*, 2020, pp. 651–660. https://doi.org/10.1109/ICUAS48674.2020.9214054.

[27] Lindner, M., Hann, R., and Wallisch, J. “UAV Icing: Numerical Simulation of Icing Effects on Wing and Empennage (Submitted).” *SAE Technical Papers*, 2023.

[28] Müller, N. C., and Hann, R. “UAV Icing: 3D Simulations of

Propeller Icing Effects and Anti-Icing Heat Loads (Submitted).” *SAE Technical Papers*, 2023.

[29] Maritime Robotics. The PX-31 Falk. https://www.maritimerobotics.com/falk. Accessed Mar. 10, 2022.

[30] Federal Aviation Administration. “Icing Design Envelopes (14 CFR Parts 25 and 29, Appendix C).” 2002.

[31] Glasheen, K., Pinto, J., Steiner, M., and Frew, E. “Experimental Assessment of Local Weather Forecasts for Small Unmanned Aircraft Flight.” *AIAA Scitech 2019 Forum*, No. January, 2019, pp. 1–10. https://doi.org/10.2514/6.2019-1193.

[32] Wallisch, J., and Hann, R. “UAV Icing: Intercycle Ice Effects on Aerodynamic Performance (Submitted).” *SAE Technical Papers*, SAE International, 2023.

[33] Barometric Formula. https://en.wikipedia.org/wiki/Barometric_formula. Accessed Apr. 2, 2023.

[34] Fajt, N., Hann, R., and Lutz, T. “The Influence of Meteorological Conditions on the Icing Performance Penalties on a UAV Airfoil.” *8th European Conference for Aeronautics and Space Sciences (EUCASS)*, 2019. https://doi.org/10.13009/EUCASS2019-240.

[35] Bratton, D., and Kennedy, J. “Defining a Standard for Particle Swarm Optimization.” *2007 IEEE Swarm Intelligence Symposium*, 2007, pp. 120–127. https://doi.org/10.1109/SIS.2007.368035.

[36] Müller, N. C., Hann, R., and Lutz, T. “UAV Icing : Numerical Simulation of Propeller Ice Accretion.” *AIAA AVIATION 2021 Forum*, 2021, pp. 1–30.

## Contact Information

Michael Cheung, Ph.D. candidate, NTNU
E-mail: man.k.m.cheung@ntnu.no

Richard Hann, Ph.D., NTNU, UBIQ Aerospace
E-mail: richard.hann@ntnu.no

Tor Arne Johansen, Professor., NTNU
E-mail: tor.arne.johansen@ntnu.no

# Appendix

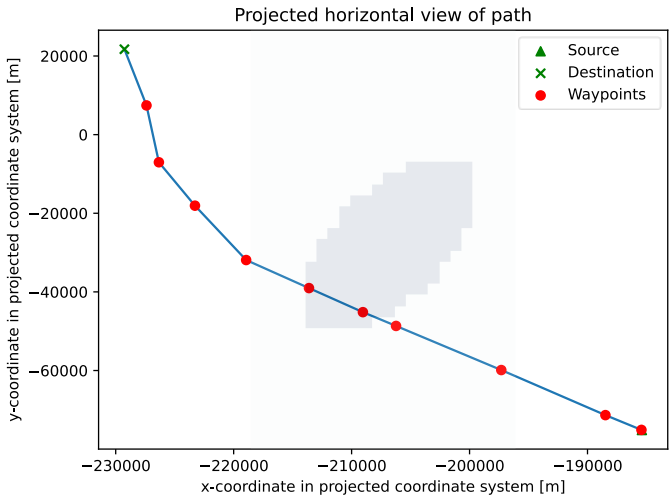


Figure 14 90-degree to path, Case 6, −2°C

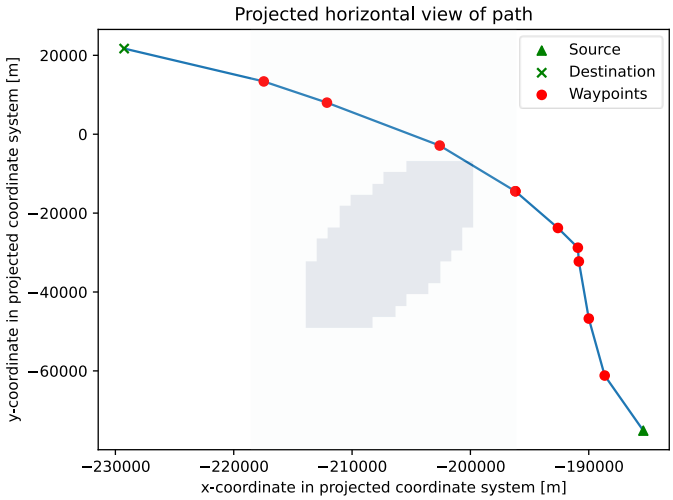


Figure 15 90-degree to the path, Case 6, −4°C

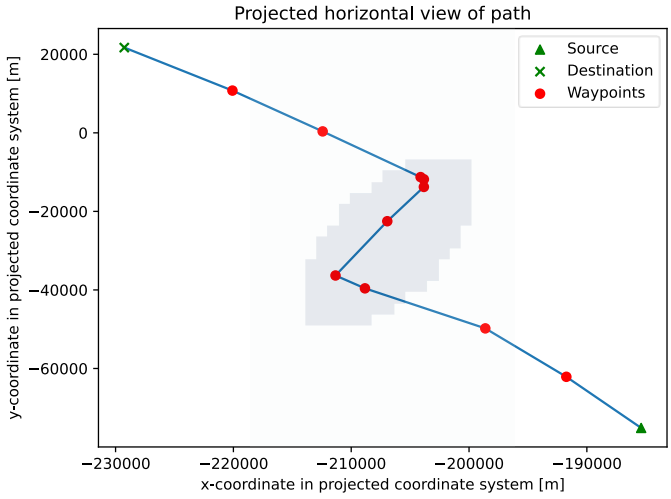


Figure 16 90-degree to the path, Case 6, −15°C

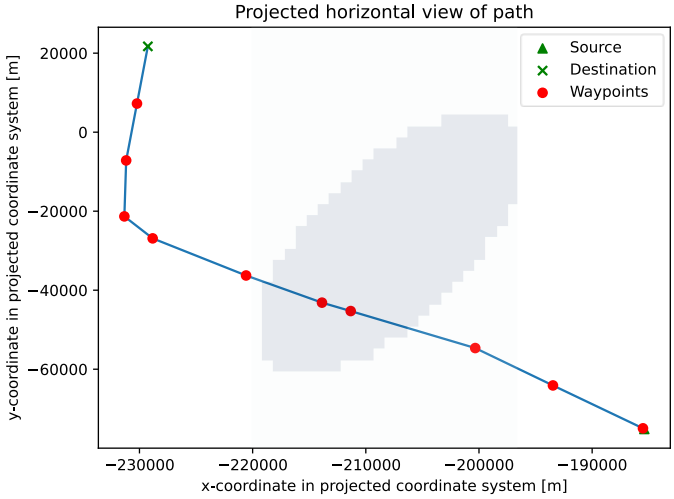


Figure 17 90-degree to the path, Case 4, −15°C

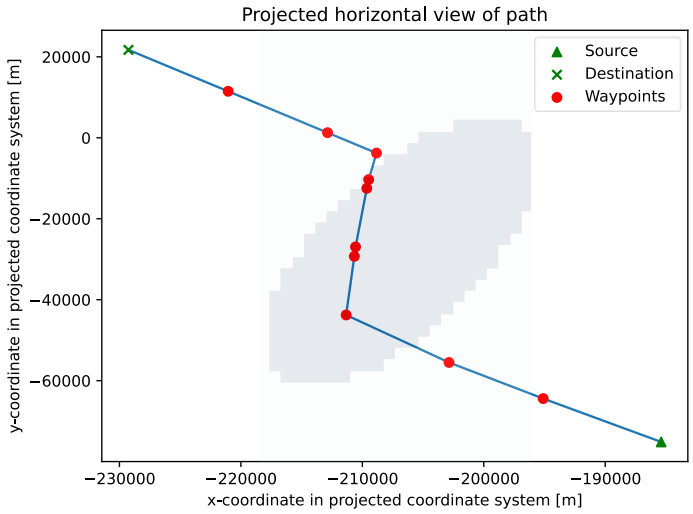


Figure 18 90-degree to the path, Case 4, -4°C

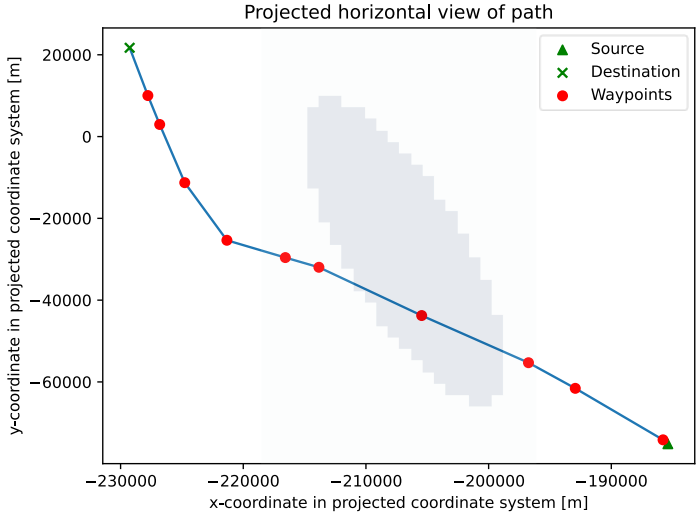


Figure 19 Along the path, Case 5, -2°C

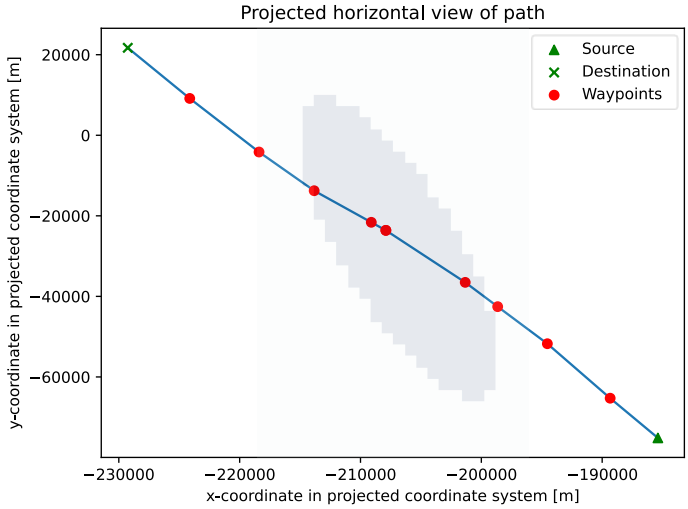


Figure 20 Along the path, Case 5, -15°C